ACS APPLIED MATERIALS & INTERFACES

Research Article

www.acsami.org

Flexible Self-Supporting Nanofibers Thin Films Showing Reversible Photochromic Fluorescence

Rui Gao,[†] Ding Cao,[†] Yan Guan,[§] and Dongpeng Yan*[,†,‡]

[†]State Key Laboratory of Chemical Resource Engineering, Beijing University of Chemical Technology, Beijing 100029, People's Republic of China

[‡]Key Laboratory of Theoretical and Computational Photochemistry, Ministry of Education, College of Chemistry, Beijing Normal University, Beijing 100875, People's Republic of China

[§]College of Chemistry and Molecular Engineering, Peking University, Beijing 100871, People's Republic of China

Supporting Information

ABSTRACT: Highly sensitive stimuli-responsive fluorescent films play an important role in smart sensors and readable optical devices. However, systems involving light-driven fluorescence changes are still limited compared with photochromic materials that simply change color upon photostimulation. Herein, by incorporation of stilbene-based molecules into a poly(vinyl alcohol) host, we have developed new flexible self-supporting nanofiber films that exhibited fast and obvious photochromic fluorescence (PCF). The reversible transfer between two fluorescent states can be easily recycled. Fluorescence microscopy and atomic force microscopy images supplied in situ evidence of changes in fluorescence and surface morphology, respectively. Density functional theoretical calculations showed that the PCF can be attributed to photoisomerization of the stilbene-based molecules. Therefore, based on the combination of experimental and theoretical studies, this work not only supplies new stilbene-based systems with light-induced fluorescence change, but also gives detailed understanding on the photoisomerization and PCF processes of the nanofibers systems. We anticipate that these PCF films can be applied in erasable memory devices and antiforgery materials, and that our strategy may be extended to other systems to fabricate multistimuli-responsive fluorescent materials.

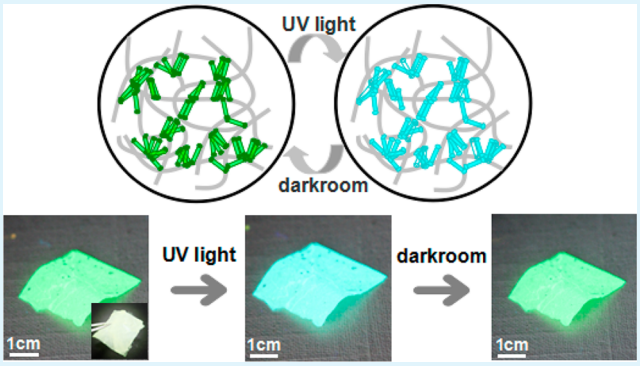

KEYWORDS: *photochromic fluorescence, nanofibers, cyanostilbene, self-supporting films, photoismerization*

INTRODUCTION

Molecule-based stimuli-responsive materials have broad applications in smart switches and sensoring devices.[1,2] In this regard, stimuli-responsive fluorescent materials have attracted considerable attention recently, because of their sensitive signal and easy imaging.[3−6] To date, several types of fluorescent switching systems sensitive to external stimuli (such as thermoinduced,[7] mechanoinduced,[8] pH-induced,[9] gas-induced,[10] and humidity-induced[11] chromic luminescent materials) have been developed; several challenges remain unresolved however. For example, for practical applications of such materials in readable/erasable intelligent systems, fast response time, high visualization contrast ratio, and stable repeatability are all required.[12−17]

Among naturally occurring external stimuli, light is one of the most common, and thus light-driven molecular responses (e.g., photochromism) have been extensively studied; several well-established photochromic molecule systems (such as azo dyes,[18] diarylethenes,[19] spiropyrans,[20] spirooxazines,[21] rhodamine,[22] and chromenes[23]) have been reported. Compared with photochromism—which solely switches the absorption spectra (i.e., color) of a chemical species between two alternative states[24]—the study of photochromic fluorescent (PCF) materials is still in its infancy, and examples are also very limited relative to other stimuli-responsive luminescent systems mentioned earlier. However, such PCF systems may pave the way to new applications in the information storage, optical communication, and antiforgery fields. Up to now, the mechanisms responsible for PCF behavior have mainly involved occurrence of chemical reactions (e.g., [2 + 2] photodimerization[14,25]) or alteration of the molecular conformation/configuration (e.g., trans−cis photoisomerization[26,27]). Due to the relatively low conversion efficiency and weak reversibility of typical solid-state chemical reactions, the latter has been recognized as the more promising way to achieve photoinduced changes in luminescence.[28,29]

Oligo(phenylenevinylene) and/or stilbene derivatives have attracted great interest for more than a half-century due to their

Received: March 5, 2015
Accepted: April 21, 2015
Published: April 21, 2015

DOI: 10.1021/acsami.5b01996
ACS Appl. Mater. Interfaces 2015, 7, 9904−9910

Scheme 1. Schematic Illustration of the Incorporation of CS Molecules (D) into PVA Fibers (B) as PCF Materials (C) Using an Electrospinning Method (A)

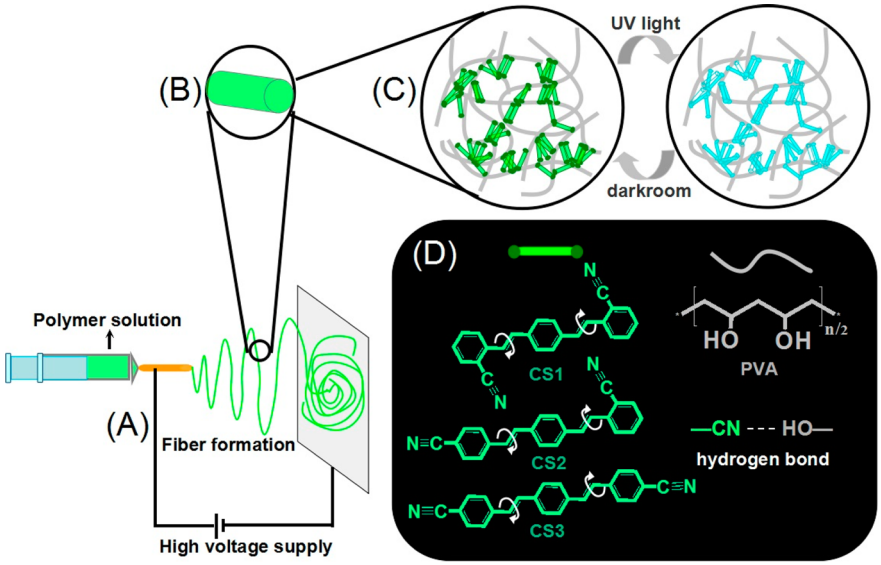

unique optical and optoelectronic properties.[30−34] It has been known that the pristine stilbene compound can exhibit trans to cis isomerization (internal rotation around a carbon−carbon double bond) upon UV irradiation.[35,36] However, how to take such an advantage toward dynamic tuning of photoinduced luminescence by controlling the orientation, stacking mode, and aggregation state of stilbene-based molecules continues a long-standing problem. Herein, we have developed new types of reversible PCF films by introducing three cyanostilbene (CS) derivatives (Scheme 1D; CS1, CS2, and CS3) into poly(vinyl alcohol) (PVA) nanofibers through an electrospinning process (Scheme 1A,B). The electrospinning method is a versatile wet technique for fabrication of continuous micro-/nanosized fibers, which can be further directly assembled into thin films.[37,38] This method has already been employed to construct polymer- and biomolecule-based films as well as inorganic/organic composites.[39−41] The choice of PVA as the electrospun matrix is based on the expectation that hydrogen-bonding interactions between -OH units in the PVA host and -C≡N groups in CS guest molecules will favor the formation of a locally ordered orientation and high dispersion of CS molecules within the fibers, leading to uniform and systematic changes in fluorescence upon photostimulus (Scheme 1C). Furthermore, the hydrogen-bonding anchoring of CS molecules within the PVA host may also enhance the photostability and reversibility of the host−guest fiber films.

The as-prepared CS@PVA fiber films present fast and obvious PCF behaviors under UV-light irradiation. The related luminescent properties of the fiber films can be easily recovered and recycled for several times. The morphological study shows that the appearances of uniformly nanosized convex structures within the fiber surface after UV irradiation, which is related to trans−cis transformation of CS molecules, is also confirmed by the theoretical calculation. Since the pristine CS-based solutions and powders have no PCF behavior at all, the transformation of PCF-free fluorophores into PCF materials by incorporation into a well-organized host−guest fiber network is the most distinctive feature of this work. Moreover, the three CS-based systems with very similar molecular structures can result in different PCF properties. Therefore, this work provides a feasible way for developing flexible PCF thin films with potential applications in luminescent antiforgery materials and photosensitive sensors.

EXPERIMENTAL SECTION

Reagents and Materials. 2-[(*E*)-2-[4-[(*E*)-2-(2-Cyanophenyl)-ethenyl]phenyl]ethenyl]benzonitrile (CS1), 1-(2-cyanostyryl)-4-(4-cyanostyryl)benzene (CS2), and 1,4-bis(4-cyanostyryl)benzene (CS3) were obtained from Sigma Chemical Co. Ltd. and used without further purification. Pol(vinyl alcohol) (PVA; M_n = 77000; 99% hydrolyzed) and hexafluoroisopropanol were purchased from Beijing Chemical Co. Ltd. and used without further purification.

Preparation of Electrospinning Solutions. Typically, 0.9 g of PVA was first dispersed into 30 mL of hexafluoroisopropanol for 2 h to obtain a PVA solution. Then, 0.09, 0.18, 0.27, and 0.36 g of CS1 (or CS2 or CS3) were added into the PVA solution under vigorous stirring. The resulting clear homogeneous solution was used for electrospinning and the fabrication of the CS@PVA films (mass concentrations, 9, 17, 23, and 29 wt %; Supporting Information (SI) Table S1).

Preparation of Electrospinning Films. A buret with an inserted Cu rod connected to a high-voltage supply was filled with the CS@PVA aqueous solution. An Al sheet connected to the ground was used as the receiver. The distance between the buret tip and receiver was fixed at 20 cm, and the high-voltage supply was fixed at 20 kV. The spinning rate was controlled at about 5 mL h^{-1} by adjusting the angle of inclination of the buret. Pieces of Al sheet about 30 cm × 40 cm were placed on the Al sheet for collecting the samples. Then, 0.5 mL of the composite solution was dropped on a clean Al sheet and left to dry under ambient conditions to form thin films.

Sample Characterization. UV−vis absorption spectra were collected in the range from 230 to 800 nm on a Shimadzu U-3000 spectrophotometer, with a slit width of 1.0 nm. The fluorescence spectra were recorded on an RF-5301PC fluorospectrophotometer with an excitation wavelength of 365 nm, with the excitation and emission slits both set to 3.0 nm. The fluorescence decays were measured using LifeSpec-ps spectrometer with a 372 nm laser exciting the films, and the fluorescence lifetimes were calculated with the F900 Edinburgh instruments software. The morphology of thin films was investigated by using a scanning electron microscope (SEM Zeiss Supra 55) equipped with an EDX attachment, and the accelerating voltage applied was 20 kV. The surface roughness and thickness data were obtained using a Bruker Multimode 8 atomic force microscope (AFM). Photoluminescence quantum yield (PLQY) and CIE 1931

DOI: 10.1021/acsami.5b01996
ACS Appl. Mater. Interfaces 2015, 7, 9904−9910

color coordinates were measured using an HORIBA Jobin-Yvon FluoroMax-4 spectrofluorimeter, equipped with an F-3018 integrating sphere. Two-photon excited fluorescence of the samples was excited by 800 nm laser on a Tsunami-Spitfire-OPA-800C ultrafast optical parameter amplifier (Spectra Physics). The fluorescence images were obtained on an Olympus U-RFLT50 fluorescence microscope.

Computational Methods. The calculations of the energy of CS-based molecules at different conformations with varying dihedral angles between adjacent phenylenevinylene units (from −180° to 180°) were performed with the density functional theory (DFT) method using the $DMol_3$ module[42] in the Materials Studio software package.[43] The initial configuration was fully optimized by the Perdew−Wang (PW91)[44] generalized gradient approximation (GGA) method with double numerical basis sets plus polarization function (DNP). The SCF convergence criterion was within 1.0×10^{-6} hartree/atom, and the convergence criterion of the structure optimization was 1.0×10^{-3} hartree/bohr.

RESULTS AND DISCUSSION

By means of the electrospinning method, CS1, CS2, and CS3 molecules were incorporated into a PVA matrix with different mass concentrations (x = 9, 17, 23, and 29 wt %) to form flexible self-supporting films CS@PVA(x%). XRD profiles for the CS@PVA show no diffraction peaks from either CS or PVA, suggesting the formation of an amorphous composite material (Figure S1 in the Supporting Information). FT-IR spectra show that the characteristic vibration bands of the cyano group in the films have systematically moved to low wavenumbers (by approximately 5−13 cm^{-1}) relative to the pure CS samples (Figure S2 in the SI), which is related to the formation of hydrogen-bonding interactions that weaken the C≡N bond. The resulting films exhibit tunable fluorescence with a red shift of the emission upon increasing the concentration of CS (Figure 1: CS1@PVA, 478−505 nm; CS2@PVA, 458−498 nm; CS3@PVA: 497−526 nm), indicating that increasing the concentration leads to the formation of *J*-type molecular aggregates and/or excimers of CS molecules within the polymer films.[13,45] The fluorescent emissions at different concentrations are uniform and homogeneous, suggesting that the CS chromophores are highly dispersed in the PVA films (inset of Figure 1).

To probe the morphological features of CS-based self-supporting films (Figure 2a), CS@PVA systems were further studied by scanning electron microscopy (SEM). It can be observed (Figure 2b) that the film is constructed from fibers with a width of ca. 200 nm. Each individual nanofiber has an extremely high aspect ratio and length, and the fiber surface is continuous and homogeneous (Figure 2c). Under a fluorescence microscope, the texture of the fibers can be clearly detected due to their strong fluorescence (Figure 2d). Further z-axis scanning images show that the fiber films feature dense three-dimensional (3D) networks composed of different orientations of fibrous aggregates (Figure 2d,e), indicating the 1D fiber nanostructures undergo self-organization and intertwining processes to afford macro-sized films. When a single fiber was excited with the excitation light polarized parallel to its long-axis direction, the emission intensities varied markedly between the parallel ($I_{\parallel}$) and perpendicular ($I_{\perp}$) polarized directions for the polarization degrees of 0°, 45°, 90°, and 135° (Figure 2f). This confirms the high-fluorescence anisotropy of the 1D nanofibers, which is related to the ordered orientation and high dispersion of CS chromophores in the PVA matrix. Moreover, the as-prepared films are highly flexible and can be easily tailored into any desired shape (Figure S3 in the SI) and thus should meet the requirements for application in soft optical devices.[46]

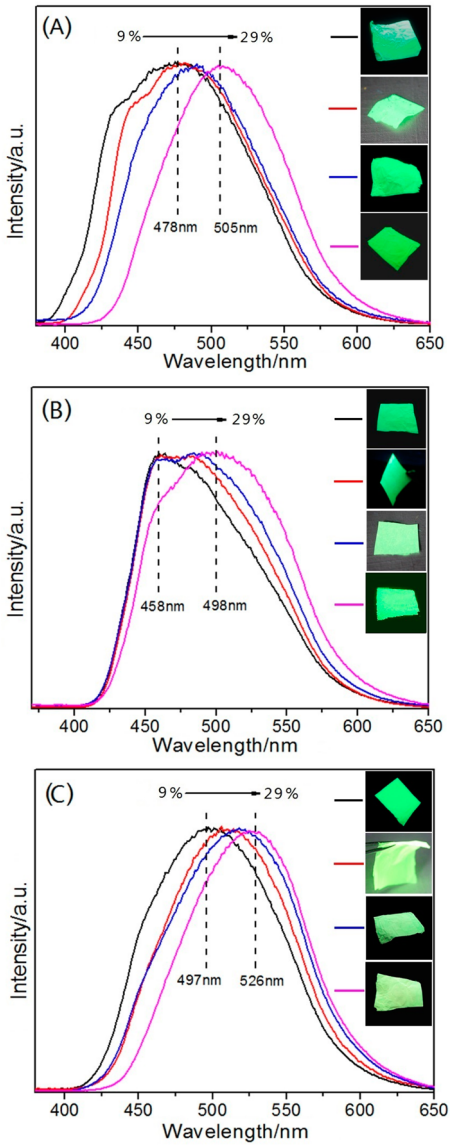

Figure 1. Fluorescence spectra of CS@PVA fiber films with different concentrations (insets show their fluorescence images under UV light): (A) CS1@PVA; (B) CS2@PVA; (C) CS3@PVA.

It was observed that all of the films underwent changes in luminescence to different extents (Table S1 in the SI) on exposure to UV light (365 nm; Xe light source, 6 W) for a very short period of time (typically less than 1 min). Such high-rate PCF has rarely been reported[48] for powder and film systems. For the CS1@PVA film, the most notable changes in both the intensity and wavelength appeared for CS1@PVA(17%), for which the maximum photoemission band (λ_{em}^{max}) moves from 484 to 441 nm with a concomitant gradual increase in the luminescence intensity (Figure 3Aa) upon UV photostimulation. The uniform change in fluorescence color is also easily visible to the naked eye (inset in Figure 3Ad). Moreover, the change can also be detected in situ for an individual fiber under a fluorescence microscope with high-power UV laser excitation (100 mW, 372 nm). It can be observed that the fluorescence color of the fibers presents an obvious change as the excitation time increases (0−20 s) (Figure 3Ac), with the corresponding

DOI: 10.1021/acsami.5b01996
ACS Appl. Mater. Interfaces 2015, 7, 9904−9910

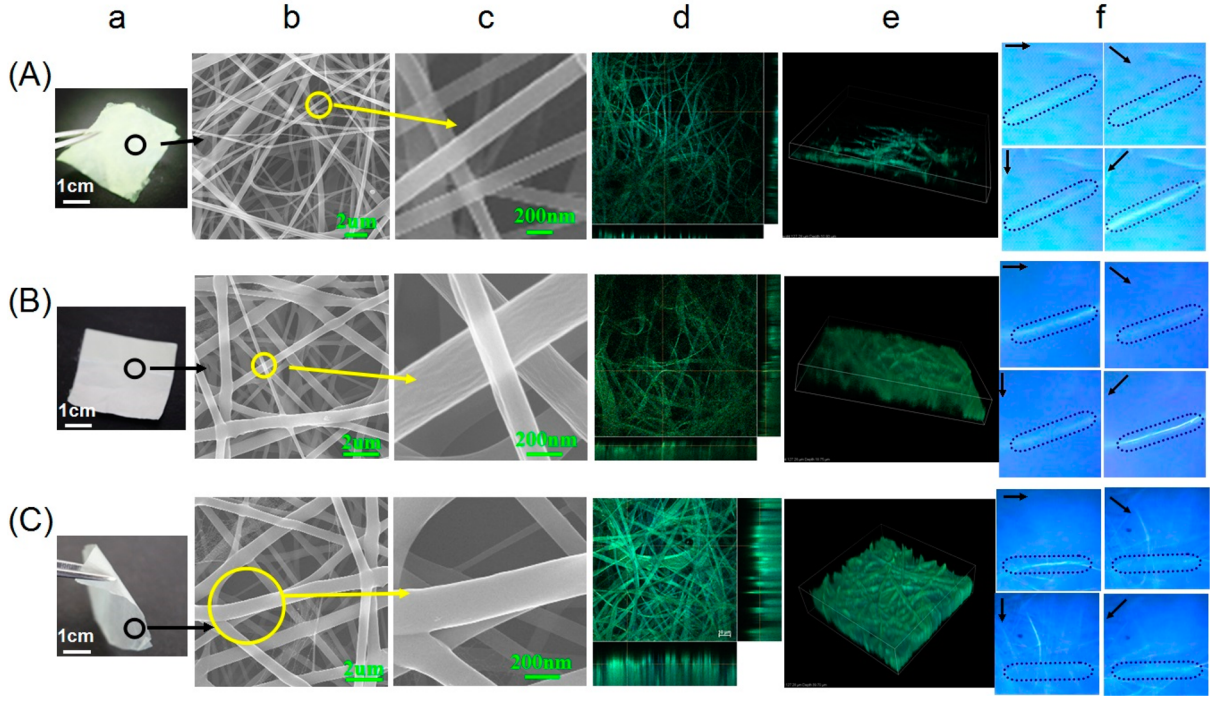

Figure 2. (a) Photographs of macrosized fiber films (a) and the corresponding SEM images (b, c); 2D and 3D fluorescence microscope images (d, e); polarized UV fluorescence microscope images (f) with the polarization directions of 0°, 45°, 90°, and 135° for individual fibers: (A) CS1@PVA(17%); (B) CS2 @PVA(23%); (C) CS3@PVA(17%).

emission color changing from green (CIE 1931 color coordinates, 0.25 and 0.47; Figure S4A in the SI) to cyan (CIE 1931 color coordinates, 0.12 and 0.52). As we have known, such in situ dynamic observation of the changes in fluorescence of a nanofiber has seldomly been reported. UV−visible absorption spectra show that the absorption bands of the fiber films exhibit a blue shift accompanied by an increase in absorption intensity below 300 nm after UV irradiation (Figure S5A in the SI), indicating a decrease in the extent of π-conjugation of the **CS1** molecules by virtue of trans−cis isomerization[47] and/or the reorganization of the molecular aggregation.[8] This conclusion is also consistent with the observed blue-shift of the fluorescence.

To obtain information about the excited states of the fiber film before and after the change in fluorescence, we measured the fluorescence lifetimes. It was observed that the fluorescence decay became much faster after UV-light irradiation (SI Figure S6A), and the corresponding fluorescence lifetime was reduced significantly from 22.4 to 10.3 ns. Additionally, the PLQY value of CS1@PVA(17%) also shows a slight decrease from 45% to 36%. Such a decrease can be attributed to the increasing molecular vibration after UV activation, which leads to an increase in nonradiative relaxation. Considering that CS molecules are potential up-conversion fluorescent materials, the up-conversion emission of the CS1@PVA(17%) film was studied using excitation by an 800 nm laser at different excitation powers (SI Figure S7A). Up-conversion emission of the film was located at 484 and 441 nm respectively before and after UV radiation, without a shift compared with those excited by UV light. Moreover, the log of the intensity has a good linear relationship with the log of incident energy, with the slope close to 2, suggesting that the emissive processes in the two luminescent states before and after the color change involve a two-photon mechanism. In addition, to compare the electrospinning films with those fabricated by other methods, CS1@PVA (17%) films were also prepared by casting and spin-coating processes and their PCF efficiency was detected. As shown in Figure S8 in the SI, for the casting film the PCF behavior is not obvious. For the spin-coating film (Figure S9 in the SI), it was observed that the film has PCF property, and the λ^{em}_{max} moves from 505 to 486 nm under UV light. Therefore, neither of their wavelength shifts is as obvious as that of the nanofibers film (ca. 43 nm). This may be related to the fact that CS-based molecules are highly dispersed for the electrospinning film, and the intertexture of electrospinning nanofibers can achieve high-efficiency absorption of the UV light.

Good reversibility and reproducibility are highly important if the films are to have practical applications as PCF materials. When the irradiated CS1@PVA film was kept in the dark for 2 h (room temperature), the fluorescence (inset in Figure 3Ad) recovered its original color and spectrum completely (Figure S10A in the SI). The reversible changes in emission (such as wavelength and intensity (Figure 3Ab)) and fluorescence lifetime (SI Figure S6A, inset) can be repeated, showing their potential for future practical sensor applications. Moreover, the fluorescence can be recovered more quickly within 0.5 h at 50 °C in the dark room, confirming that the recovery process is mainly due to thermal effects. The thermogravimetric test (Figure S11 in the SI) showed that there is a weak weight loss when the temperature is above 50 °C for the nanofibers, suggesting that 50 °C may be an optimized temperature to achieve emission recovery.

We also found similar reversible PCF occurs for both CS2@PVA and CS3@PVA fiber films, with obvious changes in luminescence (Table S1 in the SI) and absorption (Figure S5B,C in the SI) appearing after UV irradiation. For example, CS2@PVA(23%) and CS3@PVA(17%) present fluorescence blue shifts from 490 to 456 nm and from 514 to 451 nm,

DOI: 10.1021/acsami.5b01996
ACS Appl. Mater. Interfaces 2015, 7, 9904−9910

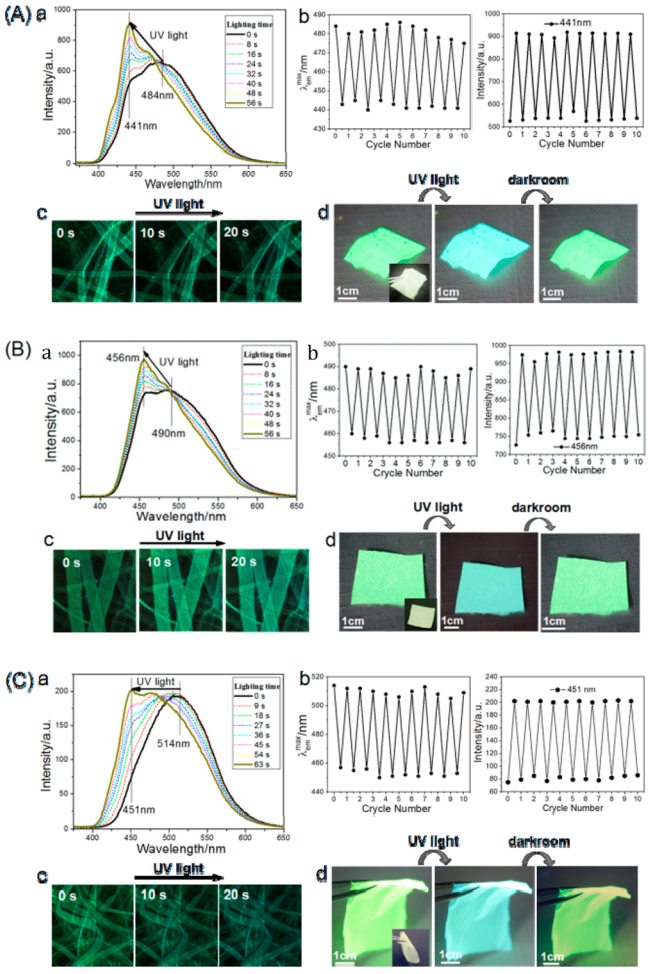

Figure 3. Fluorescence spectra (a) and fluorescence microscopy (c) of the fiber films before and after UV irradiation; the reversible fluorescence responses (λ_{em}^{max} and intensity) over five consecutive cycles (b); photographs (d) of the reversible PCF films for (A) CS1@PVA(17%), (B) CS2@PVA(23%), and (C) CS3@PVA(17%).

respectively, within 1−2 min (Figure 3B,C(a)). The color changes are accompanied by decreases in values of PLQY (Table S2 in the SI) and fluorescence lifetime (Figure S6B,C in the SI). The luminescent properties can also be recovered and recycled as shown in Figure 3B,C(b,d) and Figure S6B,C (inset) in the SI, indicating that the reversible PCF can be extended to these CS-based film systems. Moreover, it was noted that three CS molecules have a same core stilbene unit but only slightly different positions of cyano substitutents. However, the obtained CS@PVA materials present different photoemission positions and different PCF behaviors (such as different shifts in wavelength and color). Therefore, compared with the other typical PCF molecules[12] (e.g., spiropyran derivatives) that similar molecular structures present similar photochromic behaviors, this work uncovers how a slight difference in molecular structures of the photoactive isomers can result in different PCF properties. Additionally, by selective-zone irradiation of fiber films using a shadow mask, luminescent patterned films with high contrast can be easily obtained (Figure S12 in the SI), indicating that this strategy may offer a facile way to develop new luminescent patterned and/or array films with specific shapes.

The incorporation of the different CS species can result in tunable and reversible luminescent changes in the blue, green, and yellow emission regions (Figure S4 in the SI). We suggest that the reversible PCF of the three CS@PVA systems can be assigned to the reversible photoinduced change in conformation of CS molecules within the polymer matrix. The flexible PVA can supply a relatively free environment facilitating highly efficient trans−cis isomerization of the CS molecules in the amorphous aggregates. In contrast, for the pure CS-based liquid solutions and crystalline solid-state powders (Figure S13A−C in the SI), there is no PCF at all. In our opinions, for the pristine solutions (regarded as the single-molecule states), the fluorescent positions are localized in blue region (ca. 436 nm) and the light-driven molecular isomerization may not achieve an obvious fluorescence change, while for the pristine solid-state powders, the high crystal lattice energy leads to a low rotational freedom, and thus effectively inhibits the occurrence of photoisomerization. Therefore, different from the typical light-induced molecular switch systems (such as bisthienylethene and spiropyran derivatives)[12] that can exhibit PCF behaviors in both liquid- and solid-state forms, these CS-based PCF systems can only be achieved upon high dispersion into a polymer matrix. These observations confirm that the fluorescence modulation of CS systems not only involve the trans−cis isomerization of CS units at the molecular level, but also can be attributed to the change in their intermolecular interactions (i.e., the molecular aggregation) within the polymer matrix. This conclusion is also consistent with the fact that the light-induced shifts in fluorescence wavelength are highly dependent on the concentration of CS molecules in the PVA polymer as described previously. Therefore, relative to the well-known PCF systems with a mechanism based on the light-driven transformation of molecular conformation, this work may supply an alternative route to achieve PCF behaviors based on controlling the molecular configuration, stacking mode, and aggregation state.

To determine any possible morphological changes accompanying the change in fluorescence, the surface structure of the fiber was monitored in situ by an atomic force microscope (AFM) before and after UV photoirradiation. It can be observed that the pristine fiber surface is continuous and uniform with a surface roughness of ca. 13−16 nm (Figure 4A−C, left). After UV irradiation for more than 1 min, a number of nanosized spherical convex structures with a height of ca. 1 nm and diameter of 30−32 nm appeared on the surfaces of the CS@PVA nanofibers, accompanied by an increase in surface roughness (to 52−76 nm; Figure 4A−C, middle). Most of the nanosized convex structures disappeared and the surface became smooth again when the fiber film was kept in the dark for more than 2 h (Figure 4A−C, right). To better understand the reversible formation of the convex structures and concomitant reversible PCF behavior of the CS-based fibers, density functional theoretical calculations were performed on three idealized CS models to obtain the molecular energies in different conformations with varying dihedral angles between adjacent phenylenevinylene units. It was found that the most probable dihedral angles for CS1, CS2, and CS3 appear at 180°, corresponding to the low-energy trans-forms, while those for cis states are at 30°, −30°, and 90° (SI Figure S14), respectively. The calculated energy barriers for the change from trans to cis conformations are 378, 415, and 434 nm respectively for CS1, CS2, and CS3, confirming that UV light (365 nm) should result in the photoismerization of the three CS molecules in theory. Compared with the corresponding trans forms, the lengths of the *cis*-CS1, CS2, and CS3 molecules

DOI: 10.1021/acsami.5b01996
ACS Appl. Mater. Interfaces 2015, 7, 9904−9910

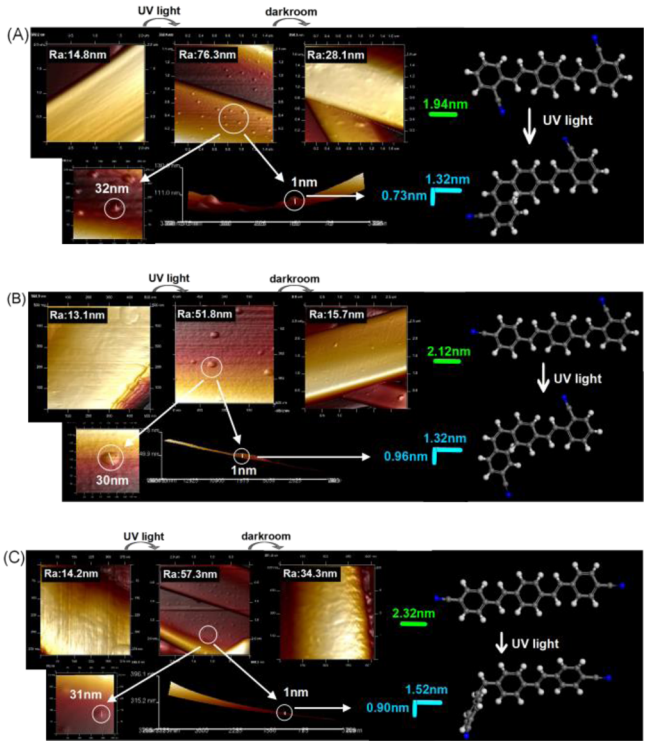

Figure 4. AFM images of fiber surfaces before/after UV irradiation (left/middle) and after recovery in the dark (right) as well as typical cis−trans molecular conformations: (A) CS1@PVA(17%); (B) CS2@PVA(23%); (C) CS3@PVA(17%).

in the short-axis direction increase by 0.73, 0.96, and 0.90 nm, respectively (Figure 4A−C). These distances are comparable to the height of the nanosized convex structures observed by AFM. Additionally, the decrease in the extent of π-conjugation in the long-axis direction on going from the trans to the cis conformation can lead to a blue shift of the absorption and fluorescence, consistent with the experimental results.

CONCLUSION

In summary, we have fabricated flexible self-supporting nanofiber film systems by the incorporation of CS molecules in a PVA matrix. Upon UV photostimulation, the fiber films exhibited fast and obvious luminescence changes (including color, intensity, PLQY, fluorescence lifetime, and two-photon emission). The reversible PCF responses promise such films can be potentially used in future high-speed readable/erasable memory devices and fluorescent antiforgery materials. Moreover, confocal fluorescence microscopy and AFM scanning were used to in situ detect changes of their fluorescence and the surface nanosized convex morphology. Theoretical calculations show that PCF properties of the fiber films are highly related to photoisomerization of CS molecules, which are also consistent with the spectra and morphological observations in experiment. It is anticipated that the incorporation of other stimuli-sensitive fluorescent molecules in flexible polymers can be utilized to fabricate a range of new smart luminescent film materials.

ASSOCIATED CONTENT

Supporting Information

(Figure S1) XRD profiles of fiber films, (Figure S2) FT-IR spectra of fiber films and pristine CS samples, (Figure S3) different shapes of fiber films under UV light, (Table S1) fluorescence spectra of CS@PVA fiber films with different concentrations before and after UV irradiation, (Figure S4) color coordinates of fiber films before and after UV irradiation, (Figure S5) UV−vis absorption spectra of fiber films before and after UV irradiation, (Figure S6) typical fluorescence decay curves of fiber films before and after UV irradiation with fluorescence lifetimes over five consecutive cycles, (Figure S7) fluorescence spectra of fiber films excited by an 800 nm laser under different pump powers before and after UV irradiation, (Figure S8) fluorescence spectra and photographs under UV light of the CS1@PVA film made by casting before and after UV irradiation, (Figure S9) fluorescence spectra and photographs under UV light of the CS1@PVA film made by spin-coating before and after UV irradiation, (Figure S10) fluorescence spectra of fiber films before and after UV irradiation over one cycle, (Figure S11) thermogravimetric curve of the CS1@PVA, (Table S2) PLQY of CS@PVA fiber films before and after UV irradiation, (Figure S12) images of the patterned array of fiber films, (Figure S13) fluorescence spectra of CS solids and liquid solutions before and after UV irradiation, and (Figure S14) molecular energies for CS molecules with different dihedral angles. The Supporting Information is available free of charge on the ACS Publications website at DOI: 10.1021/acsami.5b01996.

AUTHOR INFORMATION

Corresponding Author

*Fax: +86-10-64425385. Tel.: +86-1064412131. E-mail: yandongpeng001@163.com; yandp@bnu.edu.cn.

Notes

The authors declare no competing financial interest.

ACKNOWLEDGMENTS

This work was supported by the 973 Program (Grant No. 2014CB932103), the National Natural Science Foundation of China (NSFC), and the Beijing Municipal Natural Science Foundation (Grant No. 2152016).

REFERENCES

(1) Kobatake, S.; Muto, H.; Ishikawa, T.; Irie, M. Rapid and Reversible Shape Changes of Molecular Crystals on Photoirradiation. *Nature* **2007**, *446*, 778−781.

(2) Yao, W.; Yan, Y.; Xue, L.; Zhang, C.; Li, G.; Zheng, Q.; Zhao, Y.; Jiang, H.; Yao, J. Controlling the Structures and Photonic Properties of Organic Nanomaterials by Molecular Design. *Angew. Chem., Int. Ed.* **2013**, *52*, 8713−8717.

(3) Chan, J. C. H.; Lam, W. H.; Wong, H.-L.; Wong, W. T.; Yam, V. W. W. Tunable Photochromism in Air-Stable, Robust Dithienylethene-Containing Phospholes through Modifications at the Phosphorus Center. *Angew. Chem., Int. Ed.* **2013**, *52*, 11504−11508.

(4) Jiang, G.; Wang, S.; Yuan, W.; Jiang, L.; Song, Y.; Tian, H.; Zhu, D. Highly Fluorescent Contrast for Rewritable Optical Storage Based on Photochromic Bisthienylethene-bridged Naphthalimide Dimer. *Chem. Mater.* **2006**, *18*, 235−237.

(5) Sagara, Y.; Kato, T. Mechanically induced Luminescence Changes in Molecular Assemblies. *Nat. Chem.* **2009**, *1*, 605−610.

(6) Yoon, J. Encoding Optical Signals. *Angew. Chem., Int. Ed.* **2014**, *53*, 6600−6601.

(7) Chandrasekharan, N.; Kelly, L. A. A Dual Fluorescence Temperature Sensor Based on Perylene/exciplex Interconversion. *J. Am. Chem. Soc.* **2001**, *123*, 9898−9899.

(8) Yan, D. P.; Lu, J.; Ma, J.; Qin, S.; Wei, M.; Evans, D. G.; Duan, X. Layered Host−Guest Materials with Reversible Piezochromic Luminescence. *Angew. Chem., Int. Ed.* **2011**, *50*, 7037−7040.

DOI: 10.1021/acsami.5b01996
ACS Appl. Mater. Interfaces 2015, 7, 9904−9910

(9) Zhou, K. J.; Liu, H. M.; Zhang, S. R.; Huang, X. N.; Wang, Y. G.; Huang, G.; Sumer, B. D.; Gao, J. M. Multicolored pH-Tunable and Activatable Fluorescence Nanoplatform Responsive to Physiologic pH Stimuli. *J. Am. Chem. Soc.* **2012**, *134*, 7803−7811.
(10) Lim, S. H.; Feng, L.; Kemling, J. W.; Musto, C. J.; Suslick, K. S. An Optoelectronic Nose for The Detection of Toxic Aases. *Nat. Chem.* **2009**, *1*, 562−567.
(11) Kunzelman, J.; Crenshaw, B. R.; Weder, C. Self-Assembly of Chromogenic Dyes a New Mechanism for Humidity Sensors. *J. Mater. Chem.* **2007**, *17*, 2989−2991.
(12) Francisco, M. R.; Massimiliano, T. Electron and Energy Transfer Modulation with Photochromic Switches. *Chem. Soc. Rev.* **2005**, *34*, 327−336.
(13) Yan, D. P.; Lu, J.; Ma, J.; Wei, M.; Evans, D. G.; Duan, X. Reversibly Thermochromic, Fluorescent Ultrathin Films with a Supramolecular Architecture. *Angew. Chem., Int. Ed.* **2011**, *50*, 720−723.
(14) Papaefstathiou, G. S.; Zhong, Z.; Geng, L.; MacGillivray, L. R. Coordination-Driven Self-Assembly Directs a Single-Crystal-to-Single-Crystal Transformation That Exhibits Photocontrolled Fluorescence. *J. Am. Chem. Soc.* **2004**, *126*, 9158−9159.
(15) An, B.-K.; Kwon, S.-K.; Park, S. Y. Photopatterned Arrays of Fluorescent Organic Nanoparticles. *Angew. Chem., Int. Ed.* **2007**, *46*, 1978−1982.
(16) Furukawa, S.; Shono, H.; Mutai, T.; Araki, K. Colorless, Transparent, Dye-Doped Polymer Films Exhibiting Tunable Luminescence Color: Controlling the Dual-Color Luminescence of 2(2′-Hydroxyphenyl)imidazo[1,2-*a*]pyridine Derivatives with the Surrounding Matrix. *ACS Appl. Mater. Interfaces* **2014**, *6*, 16065−16070.
(17) Wang, X.; Wang, Y.; Bi, S.; Wang, Y.; Chen, X.; Qiu, L.; Sun, J. Optically Transparent Antibacterial Films Capable of Healing Multiple Scratches. *Adv. Funct. Mater.* **2014**, *24*, 403−411.
(18) Beyer, J. P.; Krueger, M.; Giesselmann, F.; Zentel, R. Photoresponsive Ferroelectric Liquid-Crystalline Polymers. *Adv. Funct. Mater.* **2007**, *17*, 109−114.
(19) Irie, M. Diarylethenes for Memories and Switches. *Chem. Rev.* **2000**, *100*, 1685−1716.
(20) Massimiliano, T.; Silvia, G.; Francisco, M. R. Fluorescence Modulation in Polymer Bilayers Containing Fluorescent and Photochromic Dopants. *Adv. Funct. Mater.* **2005**, *15*, 787−794.
(21) Stoll, R. S.; Hecht, S. Artificial Light-Gated Catalyst Systems. *Angew. Chem., Int. Ed.* **2010**, *49*, 5054−5075.
(22) Li, K.; Xiang, Y.; Wang, X.; Li, J.; Hu, R.; Tong, A.; Tang, B. Z. Reversible Photochromic System Based on Rhodamine B Salicylaldehyde Hydrazone Metal Complex. *J. Am. Chem. Soc.* **2014**, *136*, 1643−1649.
(23) Paul, N. D.; Mandal, S.; Otte, M.; Cui, X.; Zhang, X. P.; de Bruin, B. Metalloradical Approach to 2 H-Chromenes. *J. Am. Chem. Soc.* **2014**, *136*, 1090−1096.
(24) Terao, F.; Morimoto, M.; Irie, M. Rapid and Reversible Bending of Rodlike Mixed Crystals of Diarylethene Derivatives. *Angew. Chem., Int. Ed.* **2012**, *51*, 901−904.
(25) Tian, L.; He, F.; Zhang, H.; Xu, H.; Yang, B.; Wang, C.; Lu, P.; Hanif, M.; Li, F.; Ma, Y.; Shen, J. Thermal Cycloaddition Facilitated by Orthogonal $\pi-\pi$ Organization through Conformational Transfer in a Swivel-Cruciform Oligo(phenylenevinylene). *Angew. Chem., Int. Ed.* **2007**, *46*, 3245−3248.
(26) Feng, J.; Tian, K.; Hu, D.; Wang, S.; Li, S.; Zeng, Y.; Li, Y.; Yang, G. A Triarylboron-Based Fluorescent Thermometer: Sensitive Over a Wide Temperature Range. *Angew. Chem., Int. Ed.* **2011**, *50*, 8072−8076.
(27) Zhu, L. L.; Li, X.; Zhang, Q.; Xing, M.; Li, M. H.; Zhang, H. C.; Luo, Z.; Ågren, H.; Zhao, Y. L. Unimolecular Photoconversion of Multicolor Luminescence on Hierarchical Self-Assemblies. *J. Am. Chem. Soc.* **2013**, *135*, 5175−5182.
(28) Meier, H. The Photochemistry of Stilbenoid Compounds and Their Role in Materials Technology. *Angew. Chem., Int. Ed.* **1992**, *31*, 1399−1420.
(29) Duarte, L.; Fausto, R.; Reva, I. Structural and Spectroscopic Characterization of *E*- and *Z*-isomers of Azobenzene. *Phys. Chem. Chem. Phys.* **2014**, *16*, 16919−16930.
(30) Waldeck, D. H. Photoisomerization Dynamics of Stilbenes. *Chem. Rev.* **1991**, *91*, 415−436.
(31) Denton, G. J.; Tessler, N.; Stevens, M. A.; Friend, R. H. Spectral Narrowing in Optically Pumped Poly(*p*-phenylenevinylene) Films. *Adv. Mater.* **1997**, *9*, 547−551.
(32) Löwe, C.; Weder, C. Oligo(p-phenylene vinylene) Excimers as Molecular Probes: Deformation-Induced Color Changes in Photoluminescent Polymer Blends. *Adv. Mater.* **2002**, *22*, 1625−1629.
(33) Srinivasan, S.; Babu, P. A.; Mahesh, S.; Ajayaghosh, A. Reversible Self-Assembly of Entrapped Fluorescent Gelators in Polymerized Styrene Gel Matrix: Erasable Thermal Imaging via Recreation of Supramolecular Architectures. *J. Am. Chem. Soc.* **2009**, *131*, 15122−15123.
(34) Yan, D. P.; Delori, A.; Lloyd, G. O.; Friščić, T.; Day, G. M.; Jones, W.; Lu, J.; Wei, M.; Evans, D. G.; Duan, X. A Cocrystal Strategy to Tune the Luminescent Properties of Stilbene-Type Organic Solid-State Materials. *Angew. Chem., Int. Ed.* **2011**, *50*, 12483−12486.
(35) Fujino, T.; Arzhantsev, S. Y.; Tahara, T. Femtosecond Time-Resolved Fluorescence Study of Photoisomerization of *trans*-Azobenzene. *J. Phys. Chem. A* **2001**, *105*, 8123−8129.
(36) Liao, L.; Li, Y.; Zhang, X.; Geng, Y.; Zhang, J.; Xie, J.; Zeng, Q.; Wang, C. STM Investigation of the Photoisomerization and Photodimerization of Stilbene Derivatives on HOPG Surface. *J. Phys. Chem. C* **2014**, *118*, 15963−15969.
(37) Grafahrend, D.; Heffels, K. H.; Beer, M. V.; Gasteier, P.; Möller, M.; Boehm, G.; Dalton, P. D.; Groll, J. Degradable Polyester Scaffolds with Controlled Surface Chemistry Combining Minimal Protein Adsorption with Specific Bioactivation. *Nat. Mater.* **2011**, *10*, 67−73.
(38) Saetia, K.; Schnorr, J. M.; Mannarino, M. M.; Kim, S. Y.; Rutledge, G. C.; Swager, T. M.; Hammond, P. T. Spray-Layer-by-Layer Carbon Nanotube/Electrospun Fiber Electrodes for Flexible Chemiresistive Sensor Applications. *Adv. Funct. Mater.* **2014**, *24*, 492−502.
(39) Francesca, D. B.; Elisa, M.; Andrea, C.; Athanassia, A.; Roberto, C.; Dario, P. Photoswitchable Organic Nanofibers. *Adv. Mater.* **2008**, *20*, 314−318.
(40) Andrea, C.; Francesca, D. B.; Ripalta, S.; Antonio, A. R. N.; Roberto, C.; Dario, P. Laser Emission from Electrospun Polymer Nanofibers. *Small* **2009**, *5*, 562−566.
(41) Francesca, D. B.; Andrea, C.; Luana, P.; Anna, M. L.; Emanuela, P.; Roberto, C.; Leander, T.; Dario, P. Light-Emitting Nanocomposite CdS−Polymer Electrospun Fibres via in Situ Nanoparticle Generation. *Nanoscale* **2011**, *3*, 4234−4239.
(42) Delley, B. From molecules to solids with the DMol3 approach. *J. Chem. Phys.* **2000**, *113*, 7756−7764.
(43) *DMol3Module*, MS Modeling, Version 2.2; Accelrys: San, Diego, CA, USA, 2003.
(44) Perdew, J. P.; Chevary, J. A.; Vosko, S. H.; Jackson, K. A.; Pederson, M. R.; Singh, D. J.; Fiolhais, C. Atoms, Molecules, Solids, and Surfaces: Applications of the Generalized Gradient Approximation for Exchange and Correlation. *Phys. Rev. B* **1992**, *46*, 6671−6687.
(45) Dong, Y.; Xu, B.; Zhang, J.; Tan, X.; Wang, L.; Chen, J.; Lv, H. G.; Wen, S. P.; Li, B.; Ye, L.; Zou, B.; Tian, W. Piezochromic Luminescence Based on the Molecular Aggregation of 9, 10-Bis((*E*)-2-(pyrid-2-yl)vinyl)anthracene. *Angew. Chem., Int. Ed.* **2012**, *51*, 10782−10785.
(46) Vidyasagar, A.; Handore, K.; Sureshan, K. M. Soft Optical Devices from Self-Healing Gels Formed by Oil and Sugar-Based Organogelators. *Angew. Chem., Int. Ed.* **2011**, *50*, 8021−8024.
(47) Seo, J.; Chung, J. W.; Kwon, J. E.; Park, S. Y. Photoisomerization-Induced Gel-to-Sol Transition and Concomitant Fluorescence Switching in a Transparent Supramolecular Gel of a Cyanostilbene Derivative. *Chem. Sci.* **2014**, *5*, 4845−4850.
(48) Li, Y. N.; Urbas, A.; Li, Q. Reversible Light-Directed Red, Green, and Blue Reflection with Thermal Stability Enabled by a Self-Organized Helical Superstructure. *J. Am. Chem. Soc.* **2012**, *134*, 9573−9576.

DOI: 10.1021/acsami.5b01996
ACS Appl. Mater. Interfaces 2015, 7, 9904−9910